Splitting of valance subbands in the wurtzite *c*-plane InGaN/GaN quantum well structure

Yu Song,[a] Dong Chen, Lai Wang, Hongtao Li, Guangyi Xi, and Yang Jiang
State Key Laboratory on Integrated Optoelectronics, Department of Electronic Engineering, Tsinghua University, Beijing 100084, People's Republic of China

(Received 13 February 2008; accepted 7 October 2008; published online 24 October 2008)

Peak splitting in the low temperature photoluminescence (PL) spectra of *c*-plane InGaN/GaN single quantum well samples was observed. For the $\mathbf{k}\|\mathbf{c}$ configuration, the splitting peaks show a variation in relative intensity as the excitation power is tuned. For the $\mathbf{k}\perp\mathbf{c}$ configuration, a strong polarization dependence of the luminescence distribution and intensity was spotted. The PL spectra was analyzed with a calculation model based on the $\mathbf{k}\cdot\mathbf{p}$ effective mass theory, and the splitting peaks were identified as free-exciton transitions between the conduction subband C_1 and two groups of valence subbands, the $\{HH_1, LH_1\}$ and the $\{HH_2, LH_2, CH_1\}$, respectively. © *2008 American Institute of Physics*. [DOI: 10.1063/1.3007985]

GaN and InGaN have attracted considerable interests for the applications in the blue-green light emitting diodes (LEDs) and the laser diodes since their first realization.[1,2] In order to understand the light emission dynamics of the GaN based materials, much work has been done to analyze the emission spectra, including studying the polarization dependent optical properties of each valence band in a bulk GaN crystal.[3–6] However, very few reports on the observation of the fine valence band structure in that of an InGaN/GaN quantum well (QW) sample have been addressed so far,[7] which leaves the band structure and the optical properties of the InGaN/GaN QW an open question. The reported splitting peaks spotted in the photoluminescence (PL) spectra[8,9] vary both in the peak position and in the relative strength, and they were not attributed to the fine valence subband emissions. The lack of such reports is mainly due to the complexity in the mechanism of the optical transitions in the nitrogen containing materials, which are always under the influence of the strain induced polarization. Also they are sensitive to many parameters.[10] Studying the valence band structure and the optical properties of the InGaN/GaN QW samples is of great importance since it helps to understand the light emission mechanism and the material properties. Thus it is indicative to both material growth and device designing.

The sample used in this work was grown by the metal organic vapor phase epitaxy on *a* (0001) sapphire substrate. The epitaxial structure consists of a 3-μm-thick GaN bulk layer on top of a GaN nucleation layer, *a* strained single InGaN/GaN QW deposited at about 740 °C, and a 10-nm-thick GaN capping layer. The well structure is nominally 1.4 nm $In_{0.15}Ga_{0.85}N$/1.6 nm $In_{0.23}Ga_{0.77}N$/1.4 nm $\times In_{0.15}Ga_{0.85}N$, whose strain was controlled by optimizing the growth conditions. The stepping band profile was specifically chosen because we assume it could incorporate more subbands of QWs into the light emission based on the theoretical simulation, and at the same time avoid growing a broad well, which is known to be detrimental to the quantum efficiency. To measure the PL spectra, the sample was mounted onto the cold finger of a close-loop helium cryostat, and a 325 nm He–Cd laser with a maximum cw power of 25 mW was used as the source.

In the experiment scheme, we employed both the $\mathbf{k}\|\mathbf{c}$ and the $\mathbf{k}\perp\mathbf{c}$ configurations by rotating the sample stage to different directions. A polarizer was used to switch between the $\mathbf{E}\|\mathbf{c}$ (TE mode) and the $\mathbf{E}\perp\mathbf{c}$ (TM mode) emissions. A depolarizer is used to eliminate the polarization dependence of the spectrometer's sensitivity.[11,12]

Figure 1(a) shows the low temperature (10 K) PL spectra measured for the $\mathbf{k}\|\mathbf{c}$ configuration. No polarization dependence was observed for this configuration. The linewidth of the dominant band-edge emission peak of the InGaN QW sample is estimated to be about 35 meV, which is among the narrowest PL peak linewidths reported so far for the InGaN QW samples with a commensurate emission peak wavelength.[13,14] As is clearly resolved in Fig. 1(a), the dominant InGaN peak splits into two components, denoted as the peak (1) and the peak (2) free-exciton (FX) transition. On the lower energy side, there are a series of electron-longitudinal optical (LO) phonon coupling replicas with an equal spacing of about 90 meV.[15] It is interesting to notice the variation in the relative intensity of the peak (1) and the peak (2) emission lights measured under different excitation powers. Un-

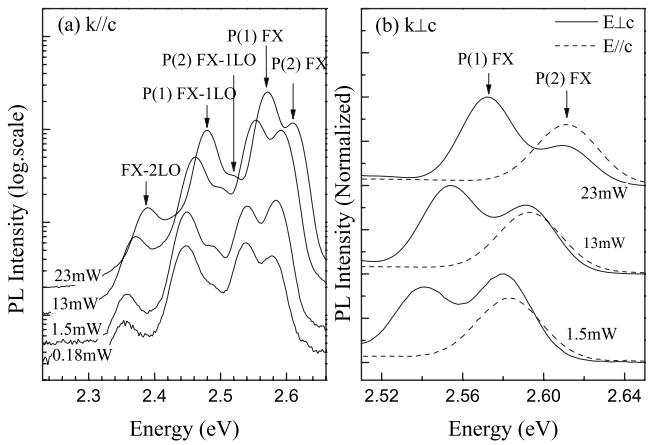

FIG. 1. The measured PL spectra for (a) the $\mathbf{k}\|\mathbf{c}$ configuration and (b) the $\mathbf{k}\perp\mathbf{c}$ configuration at 10 K. The splitting main peaks are marked as P(1), i.e., the peak (1) FX transition, and P(2), i.e., the peak (2) FX transition.

[a]Electronic mail: syskts@gmail.com.

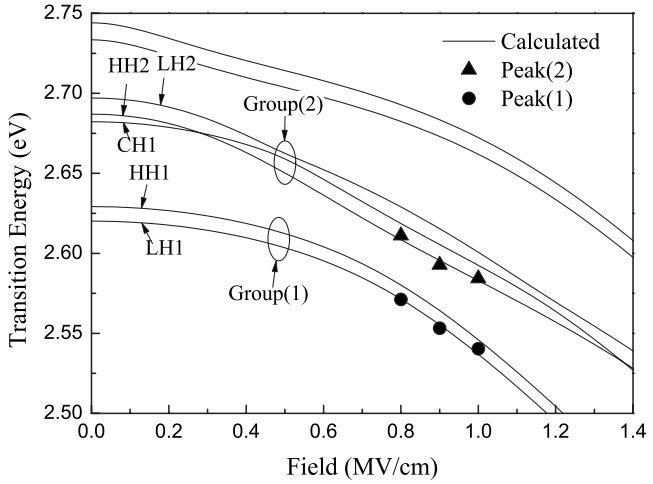

FIG. 2. The calculated transition energies at the zone center vs the electric field in the InGaN/GaN QW. Both the measured peak positions and the calculated result are depicted. The reference energy is set at E_v^0 of an unstrained GaN material.

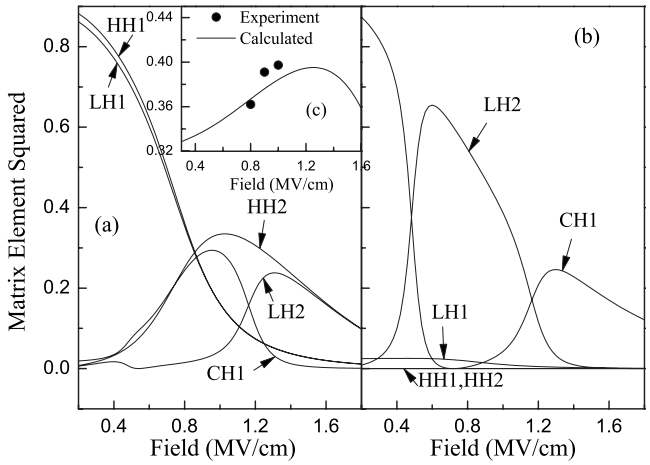

FIG. 3. The calculated (a) TE and (b) TM mode momentum matrix elements squared for the transitions between the conduction subband C_1 and the top valence subbands in the InGaN/GaN QW. The inset (c) depicts the measured and the calculated polarization degree ρ.

der excitations below 13 mW, the peak (2) FX transition is strong and is rising fast. However, under high excitations where the blueshift is significant, the intensity of the peak (1) FX transition becomes greater than that of the peak (2) transition. For the reasons to be given later in this letter, we assume that the peak (1) emission is due to the C_1-HH_1 and the C_1-LH_1 FX transitions together, and the peak (2) emission is due to the C_1-HH_2, the C_1-LH_2, and the C_1-CH_1 FX transitions together. Here C, HH, LH, and CH mean the conduction band, the heavy hole, the light hole, and the crystal-field split hole, respectively. The subscript n means the nth subband.

The result of the PL measurement in the $\mathbf{k}\perp\mathbf{c}$ configuration is plotted in Fig. 1(b). The splitting peaks of the emission are still discernable for the $\mathbf{E}\perp\mathbf{c}$ polarization, whereas the peak (1) FX transition with a lower energy vanished for the $\mathbf{E}\|\mathbf{c}$ polarization. This reveals that the peak (1) FX transition is mainly TE polarized, while the peak (2) FX transition contains both TE and TM polarized components.

Also seen in Fig. 1(b) is that the intensity of the emission is strongly polarization dependent. The polarization degree is depicted and compared with the calculation result later in Fig. 3(c). Here the polarization degree is defined as

$$\rho = \frac{I_\perp - I_\parallel}{I_\perp + I_\parallel}, \tag{1}$$

where $I_\perp$ and $I_\parallel$ are the spectrally integrated PL intensities of the $\mathbf{E}\perp\mathbf{c}$ and the $\mathbf{E}\|\mathbf{c}$ polarizations, respectively.[11]

The QW sample with double barriers used in this work was modeled with the basis-function expansion method within the $\mathbf{k}\cdot\mathbf{p}$ theory.[16–19] The band parameters used in this letter could be found in the references.[20–24] Figure 2 shows the transition energies at zone center versus the effective electric field. Transitions with the lowest energies are C_1-HH_1, C_1-LH_1, C_1-HH_2, C_1-LH_2, and C_1-CH_1. The C_1-HH_1 and the C_1-LH_1 transitions are very close in band-edge energy, with an energy gap of only 10 meV, which is much smaller than the PL linewidth of each individual emission. As a result, they should appear as one single peak in the PL spectra. And we denoted them collectively as the group (1) transitions. On the other hand, the C_1-CH_1, the C_1-HH_2, and the C_1-LH_2 transitions are very close to each other. Thus they are denoted collectively as the Group(2) transitions. It should be noted that the actual effective electric field in the QW area is induced by the piezoelectric polarization and is affected by the carrier screening, which make the effective electric field hard to determine precisely.[25] The published value varies dramatically for different samples with different structures.[25–28] Coarse estimations of the electric fields in our experiments are 1.0, 0.9, and 0.8 MV/cm for the excitation power of below 1.5, 13, and 23 mW, respectively. The measured peak positions are depicted as scatter triangles and circles in Fig. 2. We can see a good fit between the transitions of subband groups and the measured peaks.

Figures 3(a) and 3(b) depict the calculated momentum matrix elements at the zone center versus the effective piezoelectric field for the $\mathbf{E}\perp\mathbf{c}$ (TE mode) and the $\mathbf{E}\|\mathbf{c}$ (TM mode) transitions, respectively. Based on our assumption, the difference in the polarization states of the two splitting peaks observed in Fig. 1(b) could be explained through this figure. The group (1) emission is composed of the C_1-HH_1 and the C_1-LH_1 transitions both of which have strong TE mode but weak TM mode matrix elements as shown in Fig. 3. Thus it is dominantly TE polarized. On the other hand, the C_1-HH_2 and C_1-LH_2 FX transitions also have significant TE mode matrix elements, while the C_1-CH_1 transition has a strong TM mode matrix element. Thus the group (2) emission includes both TE and TM components. This is understandable considering the different origins of the valance bands from the atomic orbitals.[12,29] The drastic relative intensity variation between the C_1-LH_2 and the C_1-CH_1 is caused by the subband mixing.

The polarization degree was calculated within this theoretical framework by

$$\rho = \frac{\sum_n P_x^{C_1-\mathrm{VB}_n} - \sum_n P_z^{C_1-\mathrm{VB}_n}}{\sum_n P_x^{C_1-\mathrm{VB}_n} + \sum_n P_z^{C_1-\mathrm{VB}_n}}, \tag{2}$$

where P_x and P_z are the x (TE) and the z (TM) components of the momentum matrix element, respectively. VB_n refers to the HH_1, LH_1, HH_2, LH_2, and CH_1 subbands. The calculated polarization degree is shown as an insert in Fig. 3(c). The measured polarization degrees are also shown in this figure

as scatter dots. The good accordance again testifies our assumption that the splitting peaks observed in the PL spectra are due to the different valence subband FX transitions.

The variation in the peak (1) and the peak (2) emission intensities could also be interpreted. As is resolved in Fig. 3(a), the matrix elements of the $\Delta n=1$ transition under the electric field around 1.0 mV/cm surpasses that of $\Delta n=0$ transitions. Here it is the electric field that breaks the even symmetry of the square well potential, causing a significant decrease in the $\Delta n=0$ transition rate and making the $\Delta n=1$ transitions possible. In addition, according to the reported results,[30,31] the HH_2 and the LH_2 subbands could have a larger density of states than the HH_1 and the LH_1 subbands along the transverse direction. As a result, with the excitation power increased, it is possible for the peak (2) emission to rise fast and be relatively stronger. However when the excitation is tuned even higher, the blueshift becomes significant, which means the carrier screening becomes stronger. Thus the effective electric field is reduced along with the strength of the $\Delta n=1$ transition. As a result the relative intensity of the peak (2) emission should be suppressed, as observed in Fig. 1(a).

Also resolved in Fig. 1(a) is that the peak (1) FXs have a stronger coupling to the optical phonon in the QW sample. This is probably due to the different spatial distributions of different QW subbands. According to a recent research, the QW subband 1 FX has the greatest overlap between the phonon mode and the envelop function among all the subbands, hence it should have the most significant LO coupling.[32]

In conclusion, we have performed an analysis of the splitting peaks observed in the low temperature PL spectra of the InGaN/GaN single QW sample. Different configurations were employed in the PL experiment to measure the luminescence under different polarization directions. Calculation of the valence subband energies and the optical properties in the InGaN/GaN QW structure was carried out. The analysis provided a good interpretation of the splitting structure in the PL spectra, and the origin of the splitting peaks was accordingly identified.

This work was supported by the National Natural Science Foundation of China (Grant Nos. 60536020 and 60723002), the "973" Major State Basic Research Project of China (Grant Nos. 2006CB302801 and 2006CB302806), the "863" High Technology Research and Development Program of China (Grant No. 2006AA03A105), and the Major Project of Beijing Municipal Science and Technology Commission (Grant No. D0404003040321).

[1] S. Nakamura, T. Mukai, and M. Senoh, Appl. Phys. Lett. **64**, 1687 (1994).
[2] S. Nakamura, M. Senoh, S. Nagahama, N. Iwasa, T. Tamada, T. Matsushita, H. Kiyoku, and Y. Sugimoto, Jpn. J. Appl. Phys., Part 2 **35**, L217 (1996).
[3] D. C. Reynolds, D. C. Look, B. Jogai, A. W. Saxler, S. S. Park, and J. Y. Hahn, Appl. Phys. Lett. **77**, 2879 (2000).
[4] K. Domen, K. Horino, A. Kuramata, and T. Tanahashi, Appl. Phys. Lett. **71**, 1996 (1997).
[5] P. P. Paskov, T. Paskova, P. O. Holtz, and B. Monemar, Phys. Rev. B **64**, 115201 (2001).
[6] P. P. Paskov, T. Paskova, P. O. Holtz, and B. Monemar, Phys. Rev. B **70**, 035210 (2004).
[7] C. Wetzel, S. Kamiyama, H. Amano, and I. Akasaki, Jpn. J. Appl. Phys., Part 1 **41**, 11 (2002).
[8] J. Li, S. Li, and J. Kang, Appl. Phys. Lett. **92**, 101929 (2008).
[9] P. Perlina, C. Kisielowski, V. Iota, B. A. Weinstein, L. Mattos, N. A. Shapiro, J. Kruger, E. R. Weber, and J. Yang, Appl. Phys. Lett. **73**, 2778 (1998).
[10] Y. J. Sun, O. Brandt, M. Ramsteiner, H. T. Grahn, and K. H. Ploog, Appl. Phys. Lett. **82**, 3850 (2003).
[11] J. Shakya, K. Knabe, K. H. Kim, J. Li, J. Y. Lin, and H. X. Jiang, Appl. Phys. Lett. **86**, 091107 (2005).
[12] A. Niwa, T. Ohtoshi, and T. Kuroda, Jpn. J. Appl. Phys., Part 2 **35**, L599 (1996).
[13] G. Pozina, J. P. Bergman, B. Monemar, M. Iwaya, S. Nitta, H. Amano, and I. Akasaki, Appl. Phys. Lett. **77**, 1638 (2000).
[14] W. Shan, W. Walukiewicz, E. E. Haller, B. D. Little, J. J. Song, M. D. McCluskey, and N. M. Johnson, J. Appl. Phys. **84**, 4452 (1998).
[15] M. Smith, J. Y. Lin, H. X. Jiang, A. Khan, Q. Chen, A. Salvador, A. Botchkarev, W. Kim, and H. Morkoc, Appl. Phys. Lett. **70**, 2882 (1997).
[16] G. E. W. Bauer and T. Ando, Phys. Rev. B **38**, 6015 (1988).
[17] J. B. Xia and K. Huang, Acta Phys. Sin. **37**, 1 (1988).
[18] G. M. Sipahi, R. Enderlein, L. M. R. Scolfaro, and J. R. Leite, Phys. Rev. B **53**, 9930 (1996).
[19] S. C. P. Rodrigues, L. M. R. Scolfaro, J. R. Leite, and G. M. Sipahi, Appl. Phys. Lett. **76**, 1015 (2000).
[20] I. Vurgaftman and J. R. Meyer, J. Appl. Phys. **94**, 3675 (2003).
[21] S. K. Pugh, D. J. Dugdale, S. Brand, and R. A. Abram, Semicond. Sci. Technol. **14**, 23 (1999).
[22] J. A. Majewski, M. Städele, and P. Vogl, in *MRS Symposia Proceedings* No. 449, edited by F. A. Ponce, T. D. Moustakas, I. Akasaki, and B. A. Monemar (Materials Research Society, Pittsburgh, 1997), p. 887.
[23] D. J. Dugdale, S. Brand, and R. A. Abram, Phys. Rev. B **61**, 12933 (2000).
[24] Y. C. Yeo, T. C. Chong, and M. F. Li, J. Appl. Phys. **83**, 1429 (1998).
[25] U. M. E. Christmas, A. A. D. Andreev, and D. A. Faux, J. Appl. Phys. **98**, 073522 (2005).
[26] T. Takeuchi, S. Sota, M. Katsuragawa, M. Komori, H. Takeuchi, H. Amano, and I. Akasaki, Jpn. J. Appl. Phys., Part 2 **36**, L382 (1997).
[27] L. H. Peng, C. W. Chuang, and L. H. Lou, Appl. Phys. Lett. **74**, 795 (1999).
[28] C. Wetzel, T. Takeuchi, H. Amano, and I. Akasaki, Phys. Rev. B **61**, 2159 (2000).
[29] S. L. Chuang and C. S. Chang, Phys. Rev. B **54**, 2491 (1996).
[30] Y. C. Yeo, T. C. Chong, M. F. Li, and W. J. Fan, J. Appl. Phys. **84**, 1813 (1998).
[31] S. L. Chuang, IEEE J. Quantum Electron. **32**, 1791 (1996).
[32] D. Chen, Y. Luo, L. Wang, H. Li, G. Xi, Y. Jiang, Z. Hao, C. Sun, and Y. Han, J. Appl. Phys. **101**, 053712 (2007).